Available online at www.sciencedirect.com
SCIENCE DIRECT
Journal of Power Sources 144 (2005) 176–182
JOURNAL OF POWER SOURCES
www.elsevier.com/locate/jpowsour

Transport and electrochemical properties of the $Li_yCr_xMn_{2-x}O_4$ ($0 < x < 0.5$) cathode material

J. Molenda*, D. Pałubiak, J. Marzec

Faculty of Materials Science and Ceramics, AGH University of Science and Technology, Al. Mickiewicza 30, 30-059 Krakow, Poland

Received 19 September 2004; received in revised form 24 November 2004; accepted 29 November 2004
Available online 10 February 2005

Abstract

In this paper structural, electrical, electrochemical and thermal (DSC) characterization of series of manganese spinel samples with manganese substituted to different degree (x = 0–0.5) with chromium are presented. The conductivity and thermoelectric power measurements were performed in wide temperature range also versus oxygen partial pressure and for deintercalated samples. Electrochemical studies of these cathode materials were conducted in $Li/Li^+/Li_yCr_xMn_{2-x}O_4$ type cells. Substitution of manganese with chromium causes disappearance of the phase transition characteristic of $LiMn_2O_4$ spinel. Studies of electrical properties reveal that Cr ions do not participate in charge transport at low temperatures. In the charge curves of $Li/Li^+/Li_yCr_xMn_{2-x}O_4$ cells there are two visible plateaux, separated with distinct potential jump (∼0.5 V), which position on Li content perfectly matches the Mn^{3+} content in the doped cathode material. The lower plateau is related to the $Mn^{3+} \rightarrow Mn^{4+}$ oxidation, while the next of higher voltage, of the dopant $Cr^{3+} \rightarrow Cr^{4+}$ oxidation. The schematic diagrams of relative Mn–Cr electronic levels alignment are proposed.

Keywords: Li-ion cells; Doped manganese spinel; Cathode material; Electronic properties

1. Introduction

For several years now, the $LiMn_2O_4$ system has been attracting enormous interest as being a potential cathode material for 4 V reversible lithium batteries. Its reversible capacity equals 100–130 mA h g^{-1} and is comparable to that of the presently used $LiCoO_2$. However, manganese spinel is cheaper and more environmentally friendly. Manganese spinel undergoes a phase transition at 290 K, leading from a high-temperature cubic to a low-temperature orthorhombic phase. This transition takes place for the critical concentration of Mn^{3+} ions (Jahn–Teller ions). Most researchers attribute an insufficient number of work cycles in manganese spinel based batteries to the presence of that phase transition [1,2]. In order to extend battery life, many laboratories in the whole world have been investigating electrochemical properties of doped spinels $Li_yM_xMn_{2-x}O_4$ (M = Al, Mg, Ti, V, Cr, Fe, Co, Ni, Cu, Zn) [3–8]. These studies, however, are limited to determining lattice parameters and electrochemical characteristics. For many dopants, the charging curve changes its shape significantly, thus suggesting a modification in the electronic structure of the manganese spinel. There is a complete lack of research devoted to transport properties of doped manganese spinel. It is those properties which, to a great extent, determine the usability of a cathode material.

Electronic transport in manganese spinel $LiMn_2O_4$ at room temperature (i.e. at the working temperature of Li-ion batteries), is very difficult. A low value of conductivity, on the order of 10^{-4} S cm^{-1}, is related to the small polarons mechanism. Their migration activation energy is high, and equals 0.2–0.3 eV [9].

Previous results obtained by the authors revealed that the polaron mechanism of charge transport, in the manganese spinel, is very stable. It is not influenced by the change

* Corresponding author.
E-mail address: molenda@uci.agh.edu.pl (J. Molenda).

0378-7753/$ – see front matter © 2005 Elsevier B.V. All rights reserved.
doi:10.1016/j.jpowsour.2004.11.065

in oxygen non-stoichiometry, excess lithium in the manganese sublattice, hydrostatic pressure, or chemical intercalation [10–12].

The aim of the present paper is the determination of transport and electrochemical properties of the chromium substituted manganese spinel $LiCr_xMn_{2-x}O_4$ in the composition range of $x = 0$–0.5. Studies of electrical conductivity and thermoelectric power, performed as a function of temperature (800–1100 K) and oxygen pressure (1–10^{-4} atm), at equilibrium conditions, allowed the determination of structures of ionic and electronic defects, related to the non-stoichiometry of the oxygen sublattice. The charge transport mechanism could also be determined in a wide temperature range. The studies of structure, electrical conductivity and thermoelectric power, performed at low temperatures, together with the DSC results for doped manganese spinel, $LiCr_xMn_{2-x}O_4$, allowed the determination of charge transport mechanism in the composition range of x (0.1–0.5), and at temperatures 200–320 K, i.e. at temperatures close to the battery working temperature. Another aim of the present paper is to resolve in the electronic diagram the relative positions of manganese and chromium levels in the chromium doped manganese spinel (based on studies of electrical and electrochemical properties) in order to correlate the changes in the Fermi level position with the changes in the $Li^+/Li_yCr_xMn_{2-x}O_4$ cathode potential.

2. Experimental

2.1. Preparation of samples

Spinel compounds with a chemical composition $LiCr_xMn_{2-x}O_4$ ($0 < x < 0.5$) were prepared by solid state reaction at 800 °C. Stoichiometric amounts of Li_2CO_3, $MnCO_3$ and Cr_2O_3 were mixed in an agate mortar and synthesized in air for 24 h at 800 °C. They were grounded again in the mortar and annealed in air at 800 °C. Such obtained materials were pressed under the pressure of 10 Ton cm^{-2} to obtain pellets 1 mm thick, with a diameter of 10 mm. The pellets were annealed in air for 48 h at 800 °C and cooled rapidly down to room temperature to freeze the high temperature defect structure. X-ray studies revealed that all of the obtained spinel samples were mono-phase and had a cubic (*Fd*3*m*) structure.

2.2. XRD electrical conductivity, thermoelectric power and DSC

The XRD patterns have been measured on XRD-7 Seifert diffractometer equipped with a nickel filter and Cu Kα radiation was used. Lattice parameters were determined by the program Rayflex ver.2.286 (Rich. Seifert and Co.).

Electrical conductivity and thermoelectric power were measured at temperatures range of 220–1100 K. Standard four-probe AC method was used for electrical conductivity measurements. The pellets were shaped into elongated rectangular samples. Contacts were made with the aid of a conducting silver paste with acrylic resin as a binder.

A dynamic method was chosen for measurements of thermoelectric power. A small, growing (1–2 °C) variable temperature gradient was applied and the respective thermoelectric voltage was measured. The value of the Seebeck coefficient was calculated from an empirical dependence of voltage on the temperature gradient (linear fit with the last squares method).

High-temperature (300–1100 K) measurements of electrical conductivity and thermoelectric power were performed simultaneously on the same sample. The sample was placed in a holder between two gold plates. Two thermoelements Pt–PtRh10 attached to the plates were used to measure the temperature at the end of the sample and simultaneously to measure electrical conductivity. Two gold wires were wound around the samples to measure the voltage drop in electrical conductivity measurements. The thermoelectric power was determined by simultaneously recording of the potential and temperature changes at the ends of the sample, induced by means of an electric heater. High-temperature electrical conductivity and thermoelectric power measurements were carried out in oxygen–argon gas mixture. The oxygen pressure was determined by measuring EMF of a zirconia cell at 1070 K.

Thermal properties were studied using differential scanning calorimetry (DSC) with Mettler Toledo 821^e DSC apparatus. The sample was placed in aluminum crucibles with the empty crucible used as a reference. The measurements were performed both on cooling and heating in the temperature range 233–333 K with rates of 10 K min^{-1}.

The chemical diffusion coefficient of lithium measurements were performed by GITT technique as described by Weppner and Huggins [13].

3. Results and discussion

3.1. Electrical and thermal properties of $LiCr_xMn_{2-x}O_4$ at low temperatures

Fig. 1 shows the temperature dependence of electrical conductivity (Fig. 1a), thermoelectric power (Fig. 1b) and the DSC results (Fig. 1c, [14]) for $LiCr_xMn_{2-x}O_4$ with the chromium content of 0.1, 0.2, 0.3, 0.4 and 0.5. For comparison's sake, the characteristics for stoichiometric spinel are also shown. In the case of stoichiometric spinel, anomalous electrical and thermal effects accompany the phase transition observed at 290 K (between a cubic and orthorhombic phase) [9]. The obtained results (Fig. 1) indicate that the substitution of Mn^{3+} ions ($3d^4$) with Cr^{3+} ($3d^3$) ions results in the disappearance of the phase transition in manganese spinel. The observed activation character of electrical conductivity, together with the lack of temperature dependence of thermoelectric power, as well as its high values (on

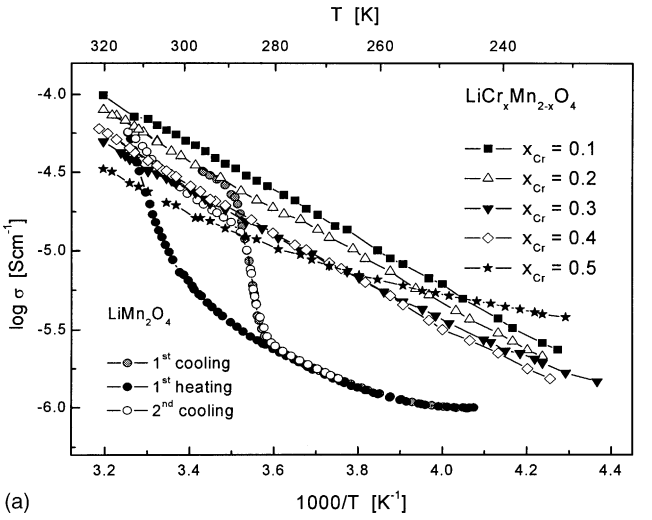

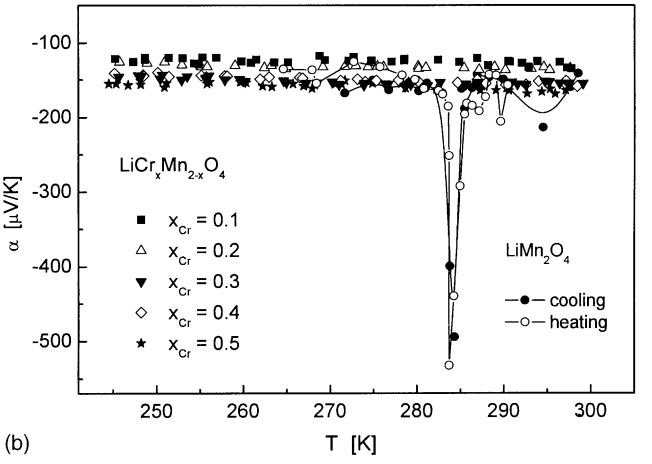

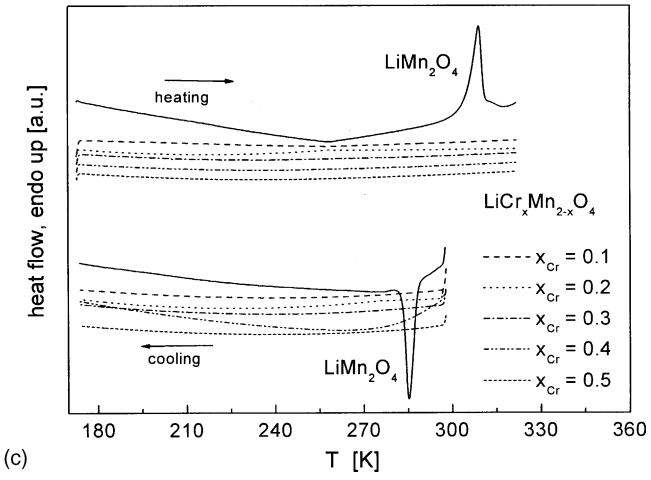

Fig. 1. Temperature dependences of electrical conductivity (a), thermoelectric power (b) and DSC (c) of the $LiCr_xMn_{2-x}O_4$.

the order of $-150\,\mu V\,K^{-1}$) indicate a polaron mechanism of charge transport, as in the case of undoped manganese spinel. It can be noticed that increasing the chromium content (Fig. 1a and b) worsens the electrical transport properties, the conductivity decreases with increasing chromium content

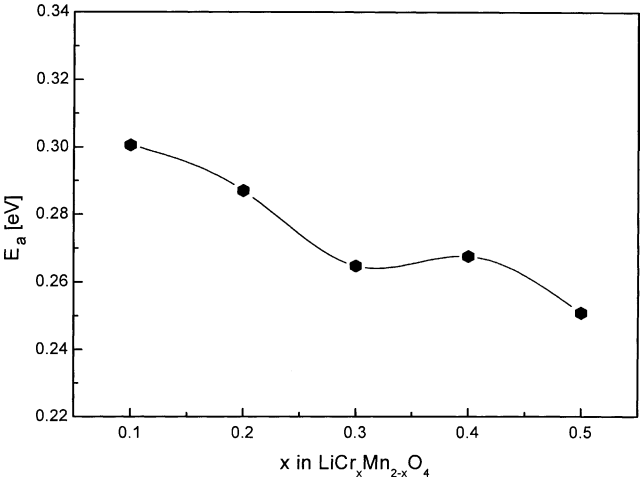

Fig. 2. Activation energy of electrical conductivity for $LiCr_xMn_{2-x}O_4$ spinel.

(0.1–0.5) by half an order of magnitude. This is related to the decrease in effective carrier concentration, which, in the case of manganese spinel (a mixed valence system) is expressed by the product $[Mn^{3+}][Mn^{4+}]$. Decreasing concentration of effective carriers is partially compensated by their increasing mobility, manifesting itself by lowering the conductivity activation energy (activation energy of carriers mobility) related to the lowering of the lattice parameter *a* with the increase in the chromium content (Figs. 2 and 3).

The presented results (Fig. 1) indicate that Cr^{3+} ions do not directly participate in charge transport at temperatures close to room temperature (working temperature of the batteries). This can be related to the configuration and positions of Mn^{3+} and Cr^{3+} ions electronic levels, shown schematically in Fig. 4.

XPS results confirm the proposed mechanism of charge transport in the chromium doped manganese spinel [14]. These results indicate that, as expected, Cr^{3+} ions isomorphically replace Mn^{3+} ions, resulting in the observed increase in average valence of manganese with increasing chromium content.

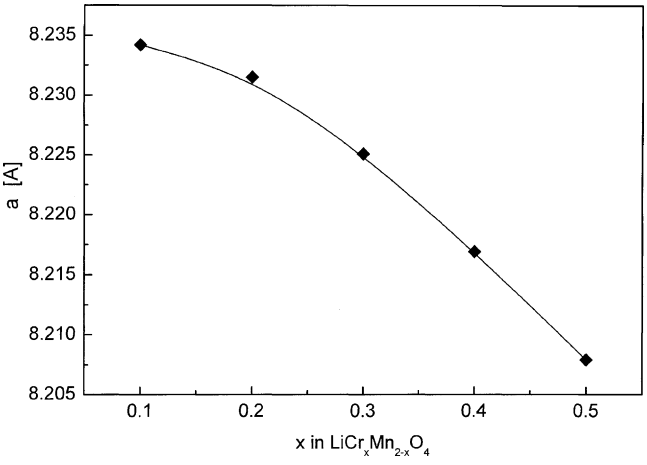

Fig. 3. Lattice parameter for $LiCr_xMn_{2-x}O_4$ spinel.

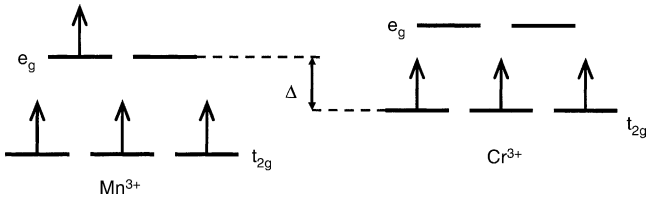

Fig. 4. Diagram of electronic levels in $LiCr_xMn_{2-x}O_4$ spinel.

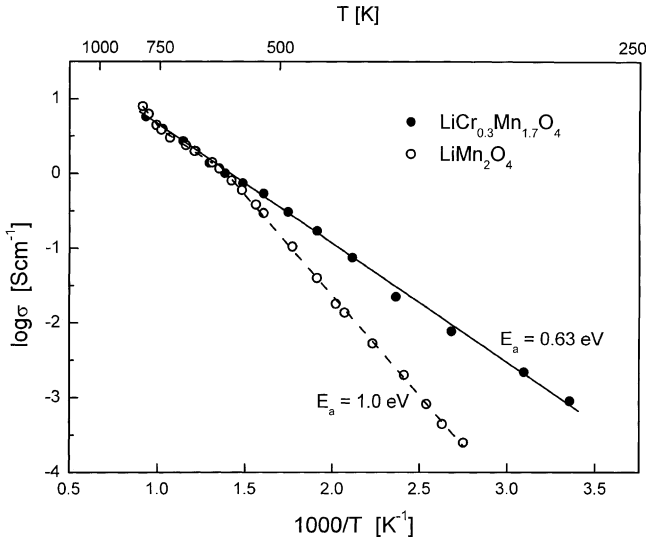

Fig. 5. Temperature dependence of electrical conductivity for chromium doped manganese spinel $LiCr_{0.3}Mn_{1.7}O_4$ in air.

3.2. Electrical properties of $LiCr_{0.3}Mn_{1.7}O_4$ at high temperatures

Figs. 5 and 6 show the temperature dependence of electrical conductivity and thermoelectric power for both, chromium doped and pure spinels in the 300–800 °C temperature range. Above 600 °C, the obtained results reflect the conditions of thermodynamic equilibrium. The character of both

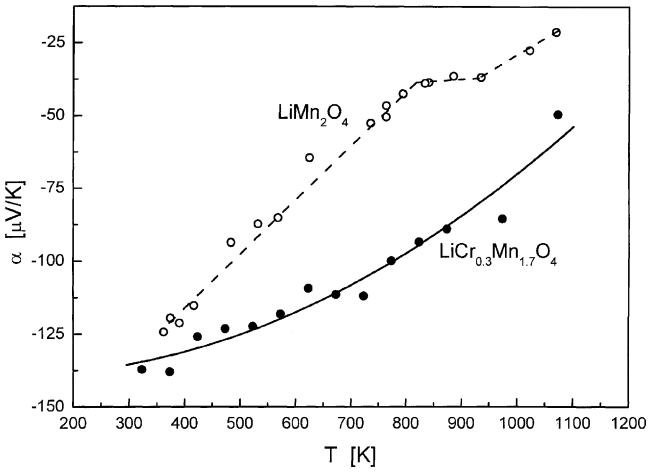

Fig. 6. Temperature dependence of thermoelectric power for chromium doped manganese spinel $LiCr_{0.3}Mn_{1.7}O_4$ in air.

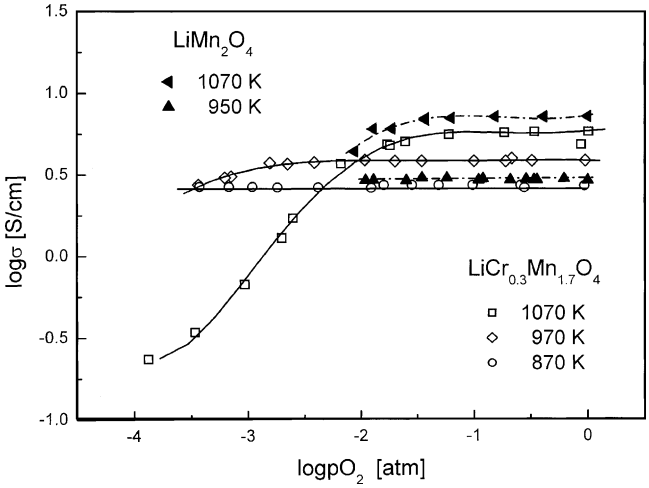

Fig. 7. Electrical conductivity as a function of oxygen partial pressure of $LiCr_{0.3}Mn_{1.7}O_4$ for different temperatures.

dependencies can be explained based on the proposed model of electronic levels (Fig. 4). The observed conductivity activation energy for the pure spinel, equalling 1 eV, corresponds to the electronic transitions $t_{2g\,Mn}$–$e_{g\,Mn}$, which is manifested by thermoelectric power approaching zero (Fig. 6). The conductivity activation energy for $LiCr_{0.3}Mn_{1.7}O_4$, equals 0.63eV, and corresponds to the transitions $t_{2g\,Cr}$–$e_{g\,Mn}$.

This means that, at high temperatures, as opposed to low temperatures, Cr^{3+} ions take part in the charge transport in manganese spinel.

Figs. 7 and 8 show the electrical conductivity and thermoelectric power for $LiMn_2O_4$ and $LiCr_{0.3}Mn_{1.7}O_4$, as a function of oxygen pressure under the conditions of thermodynamic equilibrium at several temperatures. For the chromium doped spinel, which is stable at low partial oxygen pressures, the electrical measurements were possible to be performed in wide p_{O_2} range. The effective reaction related to the oxygen sublattice non-stoichiometry (oxygen

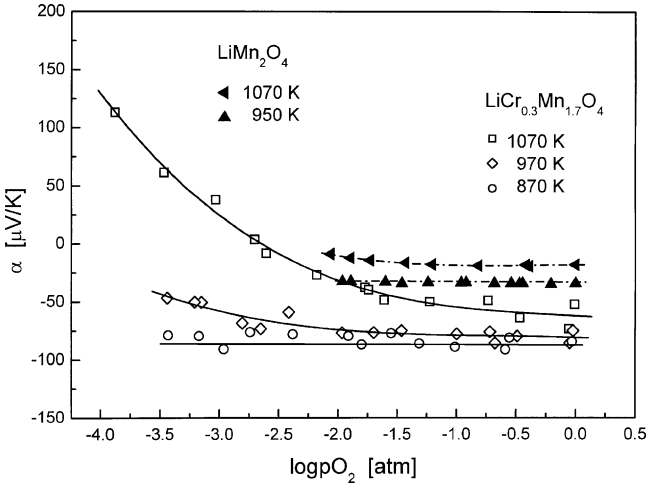

Fig. 8. Thermoelectric power as a function of oxygen partial pressure of $LiCr_{0.3}Mn_{1.7}O_4$ for different temperatures.

vacancies) is the reduction of Mn^{4+} into Mn^{3+}:

$$Mn^{4+} + e \Leftrightarrow Mn^{3+} \quad (1)$$

The lowering of electrical conductivity observed with the decrease in oxygen pressure, i.e. with increasing concentration of oxygen vacancies, being rare phenomenon in non-stoichiometric compounds (but observed, e.g. well known $YBa_2Cu_3O_{7-\delta}$) and is related to the decreasing concentration of effective carriers, what in this mixed valence compound is the product $[Mn^{3+}][Mn^{4+}]$. The measurements of electrical conductivity of $LiCr_xMn_{2-x}O_4$ at high temperatures indicate that chromium ions take part in the charge transport (activation energy equal 0.63 eV as compared to 1eV for $LiMn_2O_4$, Figs. 4 and 5). Charge transport takes place simultaneously above and below the Fermi level. Electrical conductivity may be expressed as sum of two contributions:

$$\sigma = \sigma_{Mn} + \sigma_{Cr} \quad (2)$$

Therefore, the formula for thermoelectric power is more complex and takes on the following form:

$$\alpha = \frac{\alpha_{Mn}\sigma_{Mn} + \alpha_{Cr}\sigma_{Cr}}{\sigma_{Mn} + \sigma_{Cr}} \quad (3)$$

where σ_{Mn} and α_{Mn} denotes, respectively, contributions to conductivity and thermoelectric power originating from electrons on the e_g manganese levels; similarly σ_{Cr} and α_{Cr} analogous contributions from holes on the t_{2g} chromium levels. The change of the thermoelectric power sign from negative to positive with dropping oxygen partial pressure (Fig. 8), indicates lowering of manganese conductivity contribution σ_{Mn} due to falling of effective carrier concentration, therefore, making visible the positive contribution to the total thermoelectric power related to electron holes at t_{2g} chromium levels.

3.3. *Electrochemical properties of $Li_yCr_xMn_{2-x}O_4$ ($0 < x < 0.5$)*

Fig. 9 shows the charging curves for $Li/Li^+/Li_yCr_xMn_{2-x}O_4$ batteries at the following cathode compositions: $x = 0.1$, 0.2, 0.3 and 0.4. A jump observed on the charging curve (~0.5 V) is related to a sudden change in the cathode material's Fermi level position during the lithium deintercalation process [14]. The value of the potential jump corresponds to energetic separation of t_{2gCr} and e_g levels (Fig. 4), observed also as the high-temperature conductivity activation energy of 0.6 eV (see Fig. 5). Consequently in the process of electrochemical deintercalation (charging), electrons are taken from the e_{gMn} level and then, after they are exhausted, from the t_{2gCr} level (Fig. 4). Analysis of these curves reveals that the voltage jump (its position is a function of y_{Li}) is quantitatively correlated with the amount of Mn^{3+} in the cathode material. The potential plateau of 4V is related to the oxidation of Mn^{3+} into Mn^{4+}, while that of the 5V plateau corresponds to oxidation of Cr^{3+} into Cr^{4+}. Thus, for example, in the case of cathode material having the composition

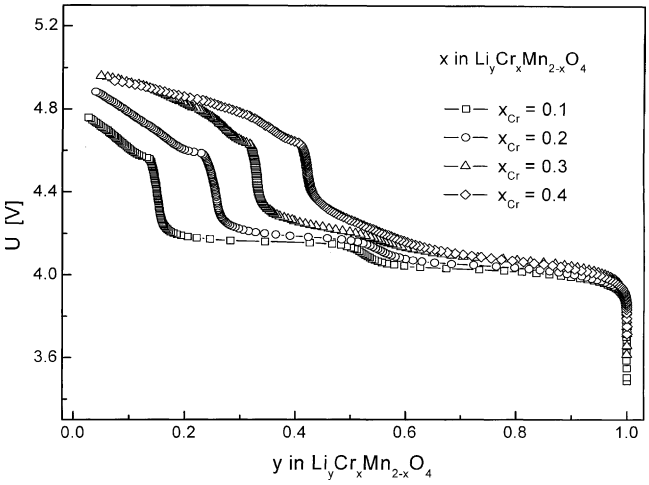

Fig. 9. Charge curves for $Li/Li^+/Li_yCr_xMn_{2-x}O_4$ cells.

$x_{Cr} = 0.1$, for which the Mn^{3+} content is 0.9 mole mole^{-1}, a jump in potential is detected at the lithium content of $y = 0.1$ (Fig. 9). The capacity for this material, in the range of 5 V, is only 0.1 mole and is related to the amount of Cr^{3+} ions. Analysis of the charging curves, shown in Fig. 9, indicates that in the case of chromium doped manganese spinel, in the range up to 0.4 mole mole^{-1}, there exists a quantitative correlation between the cathode material capacity in the range of 4 V, and the amount of Mn^{3+}.

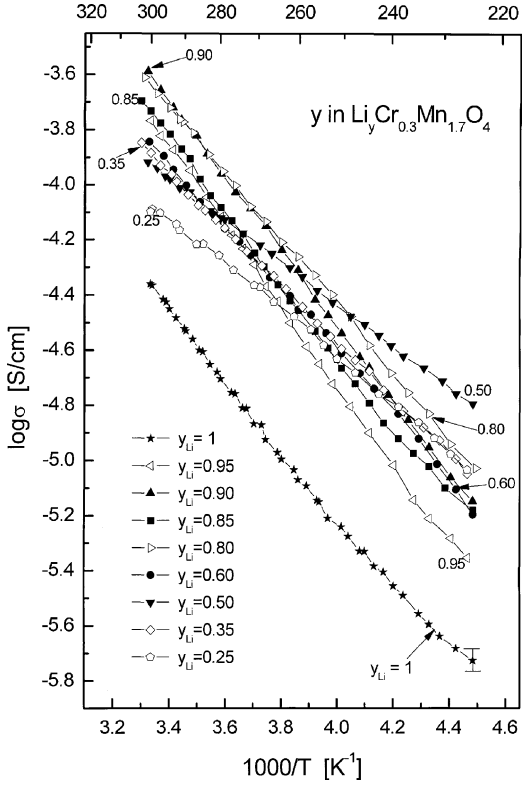

Fig. 10. Temperature dependence of electrical conductivity for deintercalated spinel $Li_yCr_{0.3}Mn_{1.7}O_4$.

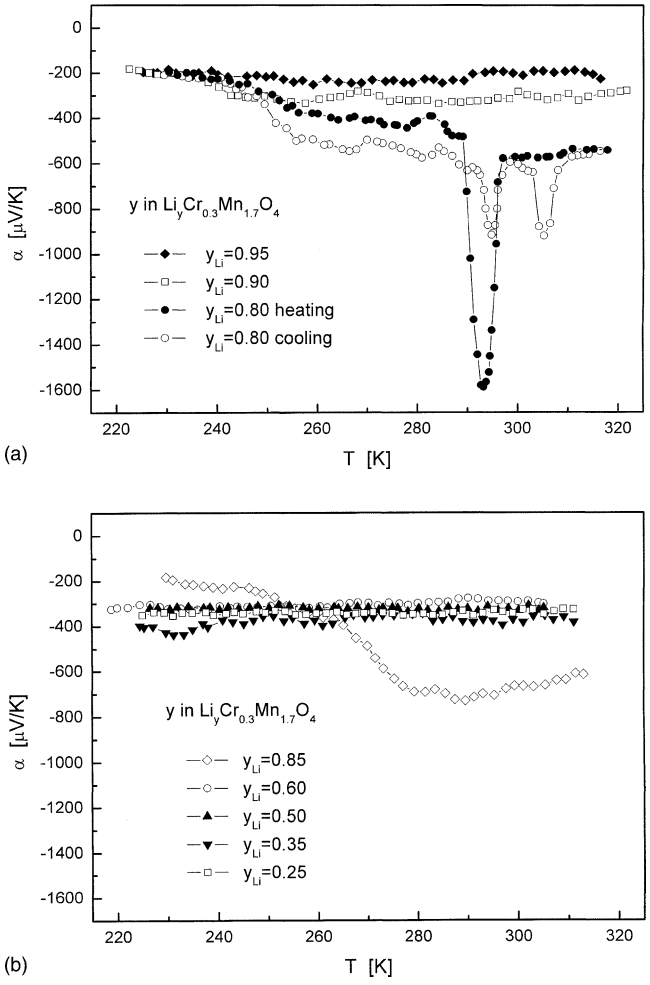

Fig. 11. Temperature dependence of thermoelectric power for deintercalated spinel $Li_yCr_{0.3}Mn_{1.7}O_4$ samples with $0.80 < y < 0.95$ (a) and with $0.25 < y < 0.85$ (b).

3.4. *Transport properties of the deintercalated $Li_yCr_{0.3}Mn_{1.7}O_4$ spinel*

Figs. 10 and 11 show the temperature dependence of electrical conductivity and thermoelectric power for deintercalated spinel $Li_yCr_{0.3}Mn_{1.7}O_4$ having a lithium content of $y = 0.95$; 0.90; 0.85; 0.80; 0.60; 0.50; 0.35 and 0.25. One can notice that with lithium deintercalation, initially electrical conductivity increases and after the dependence is not pronounced (Fig. 10). The conductivity activation energy (Fig. 12) decreases with falling lithium content, which is caused by the diminishing of the lattice parameter (Fig. 13). Measurements of thermoelectric power of deintercalated spinel $Li_yCr_{0.3}Mn_{1.7}O_4$ (Fig. 11) show the existence of strong maxima near room temperature in the sample with the lithium content of $y = 0.80$. The observed peak in thermoelectric power, of the order of 1600 $\mu V\,K^{-1}$, cannot be explained by any conventional mechanism. Similar effects were detected in the deintercalated pure manganese spinel [9], and

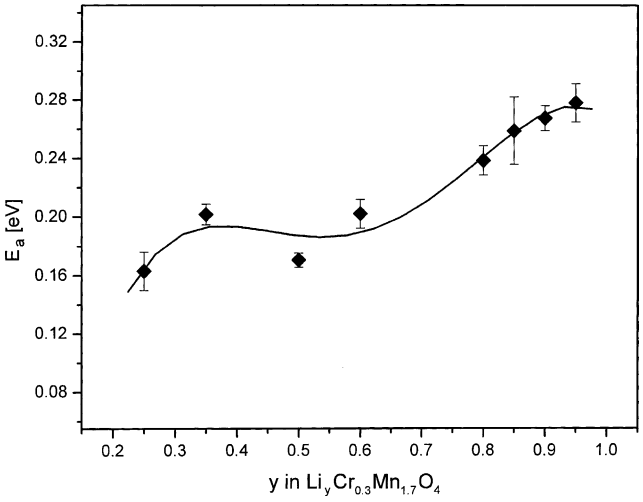

Fig. 12. Activation energy of electrical conductivity for deintercalated $Li_yCr_{0.3}Mn_{1.7}O_4$ as a function of lithium content.

also in the deintercalated spinel doped with Fe, Co, Ni and Cu [15]. The observed anomalous electronic effects indicate a high diffusivity of electrons near the Fermi level. This is important for charge transport in the process of electrochemical deintercalation/intercalation. Fig. 14 shows the results of measurements of the lithium chemical diffusion coefficient, for the deintercalated chromium doped manganese spinel $Li_yCr_{0.3}Mn_{1.7}O_4$, performed as a function of the lithium content. The obtained values of the lithium chemical diffusion coefficient, are on the order of 10^{-9}–10^{-8} $cm^2\,s^{-1}$. It is interesting to notice that for the lithium content of $y = 0.8$, when an anomalous peak in thermoelectric power was observed at room temperature, the lithium chemical diffusion coefficient (Fig. 11) has the highest value. The minimum value of the lithium chemical diffusion coefficient, observed for the lithium content of 0.4–0.55, i.e. at the end of 4 V range in the charge curve, is related to the significant deterioration of transport properties, as electrons from e_{gMn} level have all

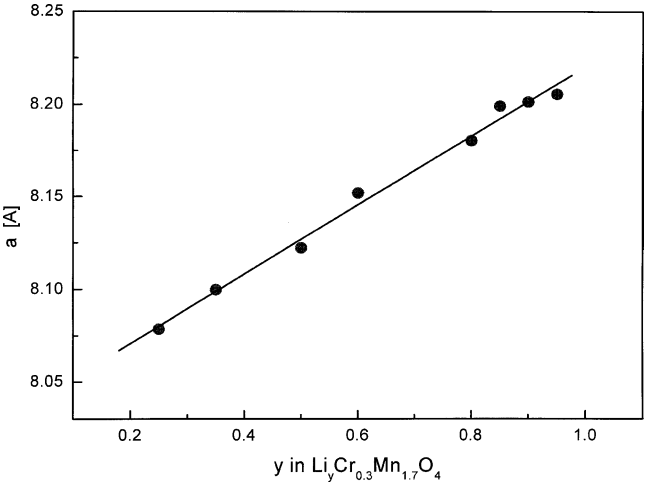

Fig. 13. Lattice parameter of deintercalated $Li_yCr_{0.3}Mn_{1.7}O_4$ as a function of lithium content.

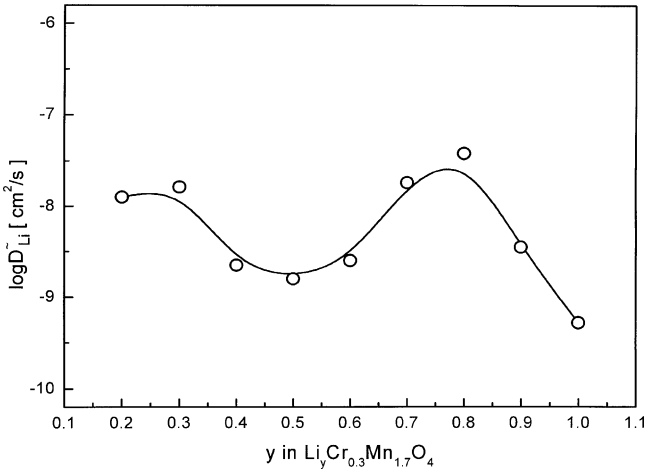

Fig. 14. Chemical diffusion coefficient of lithium in deintercalated $Li_yCr_{0.3}Mn_{1.7}O_4$.

been used up, and the transport over t_{2gCr} levels is not yet possible (Fig. 4). When the oxidation of Cr^{3+} into Cr^{4+} begins, the possibility of transport over t_{2gCr} levels appears, and the lithium chemical diffusion coefficient (ambipolar diffusion) slightly improves.

4. Conclusions

The substitution of Mn^{3+} ions with the Cr^{3+} ones, results in the suppression of phase transition in the manganese spinel. At low temperatures, chromium does not participate in charge transport. A close correlation between the amount of substituted chromium x_{Cr} and battery charging curves is related to the electronic structure of cathode material. A 4 V potential plateau corresponds to the oxidation of Mn^{3+} into Mn^{4+}, while a 5 V plateau is related to the oxidation of Cr^{3+} into Cr^{4+}. A jump in the $Li/Li^+/Li_yCr_xMn_{2-x}O_4$ battery charging curve (OCV) corresponds to the energy distance e_{gMn}–t_{2gCr}. Anomalous electronic effects in the chromium doped deintercalated spinels are related to the high efficiency of the lithium deintercalation process.

References

[1] J.M. Tarascon, W.R. McKinnon, F. Coowar, T.N. Bowmer, G. Amatucci, D. Guyomard, J. Electrochem. Soc. 141 (1994) 1421.
[2] Y. Shimakawa, T. Numata, J. Tabuchi, J. Solid State Chem. 131 (1997) 138.
[3] A. de Koch, E. Ferg, R.J. Gumuow, J. Power Sources 70 (1998) 247.
[4] Y. Shao-Horn, L.R. Middaugh, Solid State Ionics 139 (2001) 13.
[5] N. Kumagai, H. Ooto, N. Kumagai, J. Power Sources 68 (1997) 600.
[6] E. Iwata, K. Takahashi, K. Maeda, T. Mouri, J. Power Sources 81–82 (1999) 430.
[7] R. Thirunakaran, B. Ramesh Babu, N. Kalaiselvi, P. Periasamy, T. Prem Kumar, N.G. Renganathan, M. Raghavan, N. Muniyandi, Bull. Mater. Sci. 24 (1) (2001) 55.
[8] J.M. Tarascon, E. Wang, F.K. Shokoohi, W.R. McKinnon, S. Colson, J. Electrochem. Soc. 138 (1991) 2859.
[9] J. Marzec, K. Świerczek, J. Przewoźnik, J. Molenda, D.R. Simon, E.M. Kelder, J. Schoonman, Solid State Ionics 146 (2002) 225.
[10] J. Molenda, K. Świerczek, W. Kucza, J. Marzec, A. Stokłosa, Solid State Ionics 123 (1999) 155.
[11] K. Świerczek, J. Marzec, M. Marzec, J. Molenda, Solid State Ionics 157 (2003) 89.
[12] J. Molenda, W. Ojczyk, M. Marzec, J. Marzec, J. Przewoźnik, R. Dziembaj, M. Molenda, Solid State Ionics 157 (2003) 73.
[13] W. Weppner, R.A. Huggins, J. Electrochem. Soc. 124 (10) (1977) 1569.
[14] J. Molenda, J. Marzec, K. Świerczek, W. Ojczyk, M. Ziemnicki, M. Molenda, M. Drozdek, R. Dziembaj, Solid State Ionics 171 (2004) 215.
[15] J. Molenda, Solid State Ionics (2005) submitted for publication.